ON-ORBIT VALIDATION OF GYROSCOPE CALIBRATION AND OPTICAL LINK PERFORMANCE ON QUBE

René Rüddenklau [(1)], Benjamin Rödiger [(1)], Lisa Elsner [(2)]

[(1)] German Aerospace Center (DLR), Institute of Communications and Navigation, Münchenerstr. 20, 82234 Weßling, Germany, +491853282825, rene.rueddenklau@dlr.de
[(2)] Center for Telematics (ZfT), Magdalene-Schoch-Strasse 5, 97074 Würzburg, Germany

ABSTRACT

Free-space optical communication enables high-data-rate, power efficient links for small satellite missions and is a key enabler for space-based quantum key distribution (QKD). However, the narrow beam divergence of optical links imposes stringent requirements on pointing accuracy, particularly during link acquisition between space-based terminals. Unlike space-to-ground links, inter-satellite optical terminals must rely solely on onboard resources, making attitude uncertainties and misalignments between spacecraft attitude determination and control systems (ADCS) and laser communication terminals (LCTs) a challenge. The QUBE mission, which demonstrates experiments towards QKD, is used to verify LCT internal gyroscope calibration and to analyse the performance of the optical space-to-ground link. This work therefore presents the validation of an on-orbit calibration method for CubeSat-class optical terminals by aligning an LCT gyroscope with the spacecraft ADCS reference frame. Additionally, the alignment between LCT and ADCS reference frames is estimated based on high-rate tracking data from the fast-steering mirror that provides the mean offsets with respect to the satellite's body-pointing during closed-loop tracking. On-orbit pointing, acquisition and tracking results from optical downlinks demonstrate rapid acquisition times of 2 seconds, and tracking of up to 97.5% of the total operation time, equivalent to 7 minutes and 25 seconds.

1 INTRODUCTION

Satellites have become indispensable across communications, Earth observation, and scientific missions, with small satellites in particular enabling rapid and cost-efficient deployment of space infrastructure. As these spacecraft take on increasingly data-intensive tasks, radio-frequency systems are reaching their limits. Free-space optical communication (FSOC) offers a promising solution by providing high data rates, low power consumption, and reduced spectrum constraints, making it especially valuable for small satellites with limited onboard resources [1]. However, these advantages come at the cost of extremely narrow laser beam divergences up to the diffraction limit, which demands precise pointing and high attitude knowledge. In direct-to-Earth (DTE) links, relatively wide and powerful beacon beams from the optical ground station (OGS) and accurate orbit knowledge help mitigate this challenge by illuminating the satellite and reducing the search uncertainty space for the satellite laser communication terminal (LCT). In contrast, optical inter-satellite links (ISLs) must be established autonomously between terminals on two spacecraft, both operating with low-divergence beams due to limited beacon power—available on CubeSats—to extend the maximum link distance. As a result, the acquisition time increases rapidly with any uncompensated attitude uncertainty between the LCTs [2].

A challenge in current architectures is that the satellite bus and the LCT are commonly supplied by different vendors [3]. As a result, high-quality attitude information from the spacecraft's attitude determination and control system (ADCS) is often not shared with the optical payload, despite its relevance for pointing and acquisition performance. Previous work has shown that exchanging attitude knowledge between subsystems can significantly improve pointing stability. For example by feeding optical payload measurements into the spacecraft's Kalman filter to achieve sub-arcsecond stability during an active link [4]. Such techniques are particularly effective in dynamic scenarios, including high-elevation DTE passes, pointing towards OGS beacons, or maintaining accurate ISL formations. However, these approaches assume that a link is already established and optical feedback is available. During the acquisition phase, no optical feedback is present, and stabilisation typically relies solely on internal sensors, such as gyroscopes. Methods inspired by camera or gimbal control systems compensate disturbances using measured drift rates in closed-loop controllers [5], but they generally exploit only intra-gimbal sensor data and often require high-performance inertial sensors, such as fibre-optic gyroscopes, which exceed the size, weight, and power (SWAP) constraints of CubeSat-class LCTs [6]. While compact, integrated optical gyroscopes for small satellites are under development [7,8], this work focuses on commercially available micro-electro-mechanical system (MEMS) gyroscopes that can be mounted directly on the LCT's payload electronics, maintaining a fixed orientation relative to the optical axis.

An integral challenge in establishing the first link is to ensure that the coordinate systems of the LCT and the ADCS match the design. Efforts were made by the TBIRD team to measure the mounting offset before and after the rocket launch. An offset of 0.22 degrees with respect to the boresight was measured [9]. The DLR OSIRISv1 mission, which was based on pure body-pointing, determined an initial offset of 0.01 degrees [10]. State-of-the-art systems are equipped with a fine pointing assembly (FPA) to establish a field of regard (FOR) that can compensate for certain mounting offsets and disturbances. In the OSIRIS4CubeSat example, this FOR has a half-angle of 1 degree. However, an initial offset of 1.636° for the first axis and 1.066° for the second axis were measured, after extensive search pattern where executed, which led to commanded offsets in the satellite body-pointing [11]. The CLICK-A mission from MIT uses the same FOR in their LCT but did not measure any offsets [12]. Common to all examples is the fact that static offsets are known after the first link, however, there magnitude differs significantly. Additional dynamic instabilities within the body-pointing control accuracy are left unnoticed by the LCT during acquisition. Therefore, a gyroscope is proposed to propagate drift within the field-of-uncertainty from ADCS 1 Hz updates, but at the scan rate of the LCT.

The main contribution of this work is the validation of the on-orbit calibration of a MEMS gyroscope, providing a preliminary evaluation of its performance in relation to the requirements of future optical ISL missions, and assessing the robustness of the QUBE mission's links. Section 2 provides an overview of the QUBE mission, including the OSIRIS4QUBE LCT, and it briefly explains the concept of augmenting the LCT's attitude knowledge using an internal gyroscope to feed-forward body-pointing instability knowledge to the fast-steering mirror (FSM), which motivates the analysis of this device's performance during the QUBE mission. Section 3 evaluates the body-pointing errors of the satellite's ADCS, which are the foundation for the gyroscope calibration results, and additionally evaluates the optical PAT performance of 2025.

2 POINTING, ACQUISITON AND TRACKING ON QUBE

The following section highlights the QUBE mission and its relevance as a precursor mission for technology demonstration. Next, the concept of feed-forward compensation of body-pointing

uncertainties through gyroscope-supported propagation is outlined. This raises the need for gyroscope calibration and assessment of its propagation errors performed in the following section.

2.1 OSIRIS4QUBE as a Precursor for Classical and Quantum Key Distribution Missions

OSIRIS4CubeSat was the first LCT developed by DLR, especially for the purpose of providing laser communication on CubeSats [13]. This technology was intended to be used as a technology base for future developments. Especially the FPA underwent intensive testing and characterisation. This is the key technology to establish an optical connection—independent from DTE or an optical ISL—at all. The FPA has an FOR of ±1° in which the FSM can compensate residual pointing errors of the carrier platform, which is a satellite in this case. On the other hand, this means, that the platform has to point with an error less than 1° half-angle to the communication partner (OGS or other LCT). The modular approach, especially the reusability of the FPA as the core technology, enables short development times, limited qualification risks and faster technology verification in orbit. Thus, DLR is able to follow different development paths towards quantum key distribution (QKD) and towards fully operational LCTs. These can serve on different platforms like small satellites, drones and high-altitude platforms, including optical ISL and attitude independent communication using dedicated coarse pointing mechanisms.

These individual development generations allow DLR to test and verify single technologies as precursor for future missions. OSIRIS4QUBE is the first evolution of OSIRIS4CubeSat in the QKD path. With its adapted optical system, it enables technology validation of experimental QKD-signals in space [14]. The insights and gained knowledge of this mission can directly be transferred to future missions. The first iteration towards improving the classical FSOC was CubeISL, which involved extending the OSIRIS4CubeSat with an optical receiver, a modified transmitter system, and a data handling unit, in order to enable optical ISLs on CubeSats [15], which will in turn benefit from the results of QUBE.

For the QKD iteration, the lessons learned from OSIRIS4CubeSat were transferred to OSIRIS4QUBE to improve the reliability and probability of optical links. Additional technologies to increase the performance and to prepare the terminal for future missions were integrated. One example is a self-contained inertial measurement unit (IMU) consisting of gyroscopes and magnetometers to increase the pointing knowledge of the payload. The pointing accuracy of ±1° (3σ) can be met by state-of-the-art 3U CubeSat systems as demonstrated in Section 3.1. However, for optical ISLs a pointing knowledge of ±0.1° (3σ) or better is necessary to allow fast and reliable acquisition [2].

2.2 Attitude Knowledge Augmentation Concept of the Laser Communication Terminal

An optical ISL on CubeSats places stringent demands on attitude control, since even minor pointing errors can result in the narrow optical beam divergence being exceeded. Current 6U platforms demonstrate that attitude knowledge is typically more precise than achievable pointing accuracy, with control stability often limited with respect to the optical system by micro-vibrations, mounting offsets between the body and optical frames, and instability drift accumulating between ADCS control updates. These effects distort search trajectories and significantly reduce the acquisition probability, once the spacecraft's field-of-uncertainty approaches or exceeds the terminal's FOV. To address this, the proposed attitude-augmentation concept with feed-forward compensation of body-pointing uncertainties [18] enables tighter coupling between the ADCS and the optical terminal in the absence of an optical reference signal on the quadrant-photo-diode (QPD) as depicted in Figure 1.

High-rate propagation—driven by onboard inertial sensors and periodically re-initialised using the ADCS state estimate—provides a refined attitude estimate at the temporal resolution required by fast scanning patterns used in optical ISLs. This propagated estimate serves as a feed-forward correction to the FSM, effectively compensating for short-timescale disturbances that the baseline body-pointing

cannot reject. By aligning sensor reference frames through prior calibration, and by leveraging high-rate gyroscope data (or other fast-sampling sensors), the concept reduces pattern distortion during acquisition, thereby increasing the robustness of CubeSat optical links without relying on major hardware modifications.

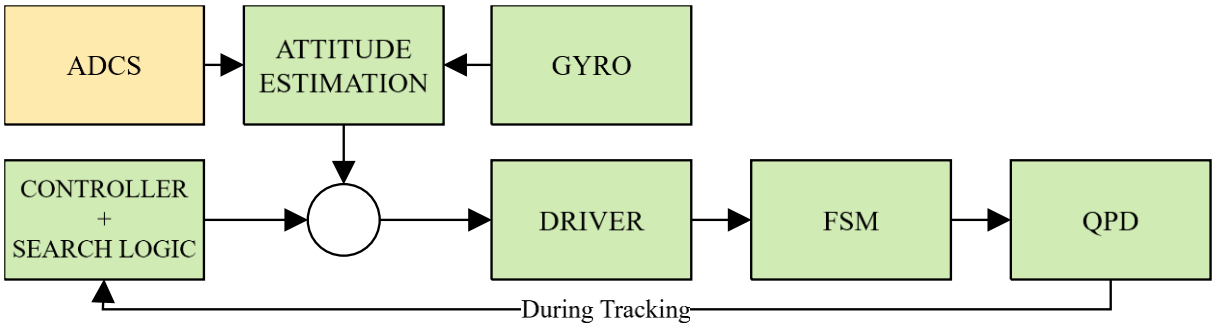

Figure 1. When gyroscope and ADCS coordinate frames are calibrated with respect to each other, gyroscope data can be used to propagate ADCS attitude estimation within the LCT [18].

In addition, the acquisition process can be further accelerated by estimating the static mounting offset between the LCT and the spacecraft bus. Mechanical tolerances inevitably cause small misalignments between the as-built hardware and the CAD reference frame, and if this offset places the optical axis outside the terminal's nominal field-of-uncertainty, the initial acquisition time can increase substantially. This offset can be identified by comparing the pre-calibrated gyroscope measurements of the LCT, expressed in the FSM frame, or the FSM offsets themselves after a successful initial link, against the corresponding ADCS inertial data.

From these data, an estimated rotation matrix can be constructed whose deviation from the theoretically modelled designed transformation reveals the true installation bias. Incorporating this offset estimate during acquisition ensures that the search pattern begins closer to the actual target direction, significantly reducing the time to establish the link.

3 ON-ORBIT PERFORMANCE ANALYSIS

The following section briefly discusses the results of the on-orbit body-pointing performance of the satellite with respect to a given attitude knowledge. The attitude knowledge is used as a reference to calibrate the gyroscope of the LCT on-orbit, which is necessary for the feed-forward compensation concept proposed for CubeISL as described in Section 2.2. Finally, the optical PAT performance of the 2025 links is analysed.

3.1 QUBE Attitude Determination and Control System Accuracy

The ADCS of QUBE provides the inertial pointing performance required for the optical laser experiments [4]. During ground station tracking, a time-dependent reference attitude is generated using GNSS-based orbit information and the known OGS coordinates. This results in a continuously varying inertial target that must be tracked accurately, particularly during high-elevation phases where angular rates increase significantly [16].

Attitude determination is performed using star tracker measurements fused with gyroscope data, ensuring high absolute accuracy while enabling continuous state propagation during temporary star tracker outages. Attitude control is realised via a three-axis reaction wheel configuration, with magnetorquers used for momentum management. The control system is based on a quaternion-based feedback controller that directly processes attitude and angular velocity error within a unified control

law. This approach provides stable reference tracking and disturbance rejection without the need for a cascaded attitude and rate loop architecture [4].

The residual control error of the ADCS directly affects the optical tracking performance, as remaining inertial misalignments must be compensated by the FSM within the optical terminal. In this architecture, the ADCS provides low-frequency, large-amplitude corrections, while the FSM compensates higher-frequency, small-amplitude disturbances. A stable inertial platform therefore reduces the dynamic load and saturation risk of the FSM.

Three representative in-orbit control error plots for optical experiments are shown in Figure 2, Figure 3 and Figure 4. The corresponding passes were conducted on the 2nd of May 2025 (maximum elevation 67.75°), the 13th of May 2025 (48.03°), and the 13th of August 2025 (19.88°), respectively [16]. Each graph presents the attitude control error for all three body axes of the satellite together with the star tracker validity flag.

Figure 2 corresponds to the pass with the highest maximum elevation. During this experiment, slightly increased control errors can be observed, particularly during the high-elevation phase where satellite angular rates are at their highest. Nevertheless, the residual error remains mostly below ±0.2° for the axes relevant to the optical pointing direction, which are the x-axis and y-axis.

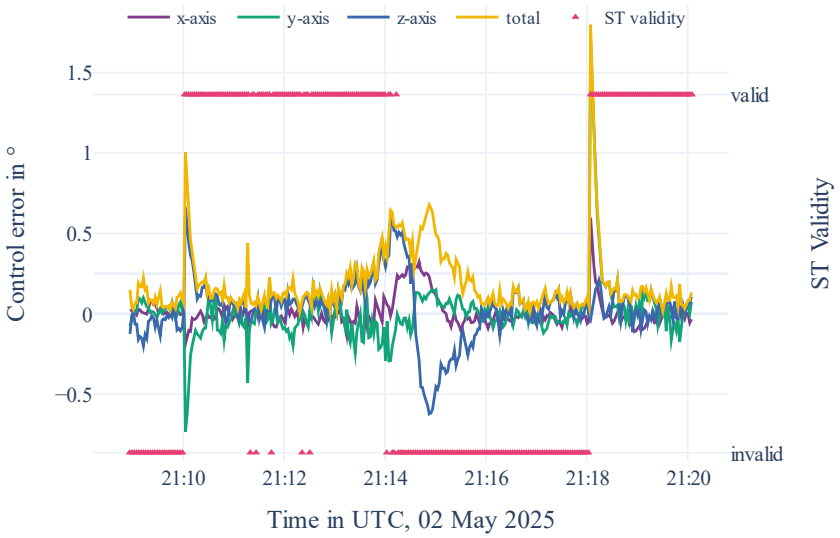

Figure 2: In-orbit ADCS control error during optical experiment on the 2nd of May 2025 (maximum elevation 67.75°) with indicated star tracker validity.

Figure 3 shows a medium-elevation pass with less demanding tracking dynamics. The control error remains well within ±0.2° for most of the tracking period. A temporary star tracker outage can be identified by the validity flag. However, there is no immediate degradation in control performance during this interval, due to the use of gyroscope-based state propagation within the attitude filter.

Figure 4 represents a low-elevation pass with comparatively low angular rates. Accordingly, the control error remains at a low level throughout most of the experiment. A short, transient peak is visible in the data and is currently under investigation, as it cannot yet be conclusively attributed to a specific disturbance source.

Across all three figures, periods of star tracker unavailability do not immediately result in increased control error, which is, however, based on the attitude knowledge estimation itself. During these intervals, the attitude estimate is propagated using ADCS only internal gyroscope data. Secondary absolute sensor data, like magnetometer, were not used, based on the lessons learned from the PIXL-1 mission. The indications of actual errors with respect to the optical axes are discussed in Section 3.3. Once the star tracker provides valid measurements again—typically after angular rates decrease—a sudden adjustment in the control error can be observed. This step-like behaviour reflects the accumulated drift of the propagated attitude estimate during the outage period. The magnitude of this correction depends on the duration of the outage and the gyroscope bias stability.

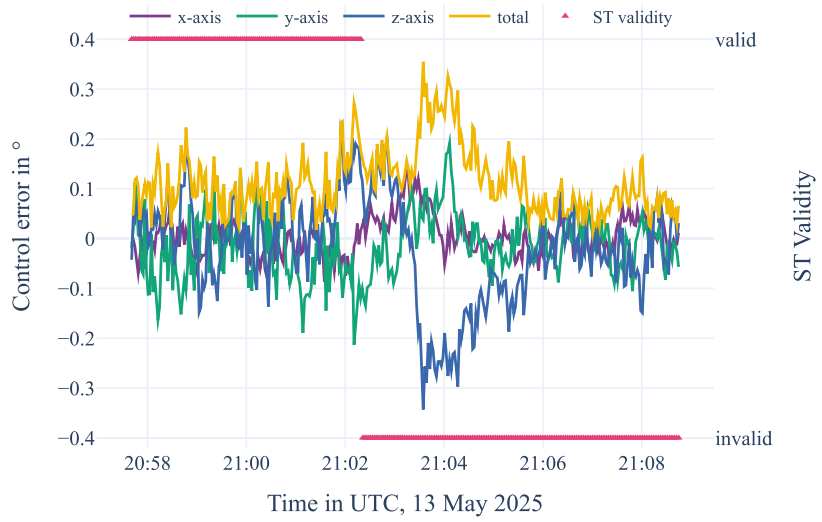

Figure 3: In-orbit ADCS control error during optical experiment on the 13th of May 2025 (maximum elevation 48.03°) [17] with indicated star tracker validity.

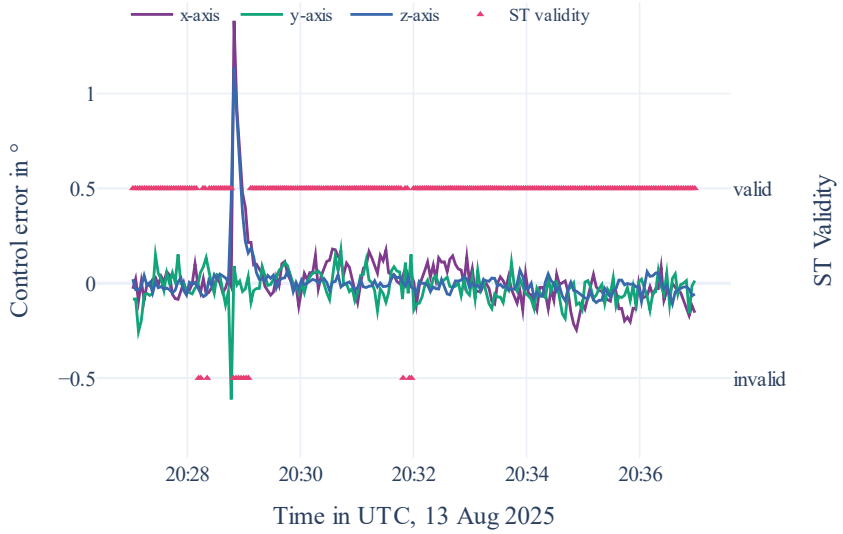

Figure 4: In-orbit ADCS control error during optical experiment on the 13th of August 2025 (maximum elevation 19.88°) with indicated star tracker validity.

Overall, the residual control error remains predominantly below ±0.2°, particularly for the axes determining the optical pointing direction. Rotation about the optical boresight is of lower relevance

for link performance, as it does not affect the alignment of the pointing axis towards the ground station when no point ahead angle is used. The results demonstrate that the ADCS provides a sufficiently stable inertial platform, limiting the dynamic load on the FSM and reducing the risk of saturation during optical experiments.

3.2 Gyroscope Calibration Results

MEMS-based gyroscopes are subject to measurement errors. There are both bias and scaling errors, which can vary depending on the device. However, these can be determined using known methods such as least-squares optimisation [19]. Ideally, the gyroscope should therefore be calibrated on the ground against a known reference, which can later be transformed to any coordinate system. It is also important to ensure that the calibration is carried out under different environmental conditions, as discussed in the results below. The coordinate system of the FSM is a good choice of reference for an LCT. However, the relatively small angular changes that are present during closed-loop tracking make it difficult to calibrate the gyroscope against this reference. However, using an established link, the calibration can also be performed in-orbit with respect to the optical system. Due to the novelty of this estimation algorithm, no ground calibration was performed for OSIRIS4QUBE. However, despite this circumstance, the significance of the estimation can still be demonstrated.

A data set from a tumbling phase of the satellite and two data sets from overflights were used as a basis for on-orbit calibration. The data was recorded simultaneously at the LCT (raw and calibrated) and at the ADCS (reference) (see Figure 5b), where the x-axis and the z-axis belong to the optical pointing direction in the local gyroscope coordinate system. Furthermore, temperature fluctuations were recorded but not taken into account during this study, as shown in Figure 5a. For all considered measurements, there is a temperature range between $-3°C$ and $+15°C$. It can be seen that the temperature of the sensor placed on the high-power laser diode (HPLD) generally increases faster than that of the sensor on the microcontroller unit (MCU), which is the expected behaviour due to thermal dissipation. It is also visible that, for links from August onwards, the temperature of the HPLD rises faster than before this date. This is accounted for an increased laser power, which was configured from previously 30 mW at the fibre output to 72 mW in June 2025.

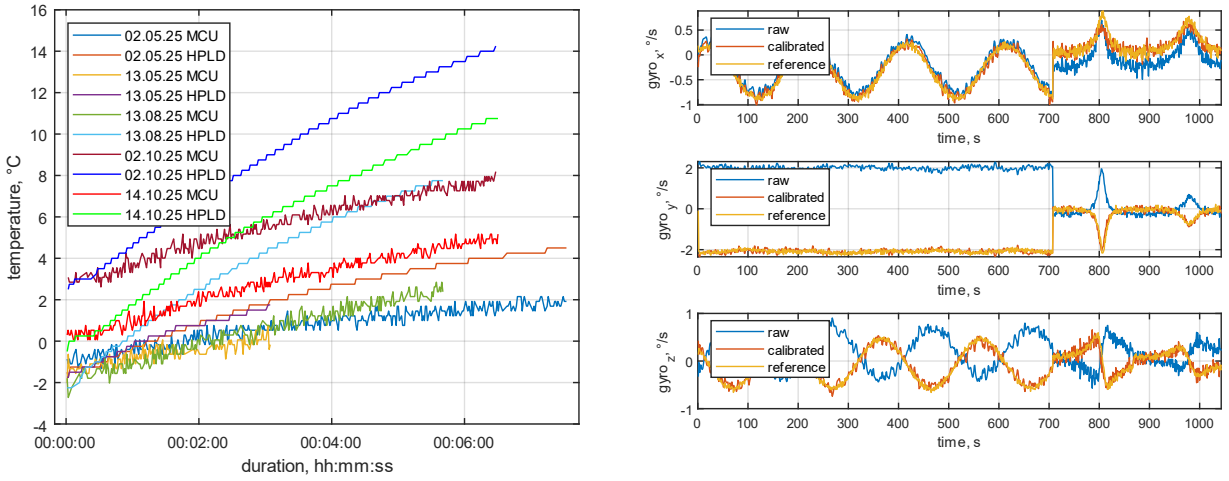

(a) (b)

Figure 5. (a) Temperature recordings at the MCU and the HPLD with laser power settings of 30 mW and 72 mW and (b) concatenated gyroscope measurements from three measurement sets ranging from May to October.

Using the above measurement set, the general calibration was found to be

$$C_{gyro} = \begin{bmatrix} 1.0035 & -0.1611 & -0.0281 \\ -0.0209 & -0.9263 & -0.0379 \\ -0.0053 & -0.0011 & -0.9419 \end{bmatrix}; b_{gyro} = \begin{pmatrix} -0.0043 \\ 0.0039 \\ -0.0020 \end{pmatrix},$$

which leads to computed RMS errors for the general calibration with respect to the reference of 0.18 °/s for the 2nd of May, 0.14 °/s for the 13th of May and 0.23 °/s for the 13th of August, and for the link specific calibration, RMS errors of 0.13 °/s, 0.12 °/s and 0.11 °/s respectively, which are the optical links analysed in Section 3.3. Based on these measurements, Figure 6 summarises the values from the gyroscope calibration and the optical tracking tests.

The actual estimated alignment is derived from the mean errors of the FSM angles with respect to its central position with three standard deviations σ based on the three individual links, and indicated with the dashed lines. Additionally, based on the found calibration, the RMS propagation error of one second of gyroscope integration is marked with an uncertainty area. It can be seen that the general calibration that, which does currently not account for temperature changes and is sampled with only 1 Hz, lies outside the FOV of the LCT. However, the link specific calibration shows that, when accounting for additional dynamic calibration errors [18], an accuracy at about the size of the FOV could be maintained. Therefore, after applying the mean offset found between the body frame and the LCT frame, as well as a calibration that accounts for dynamic effects, the gyroscope measurements can be used to propagate the ADCS attitude within 1 Hz update intervals. This maintains the correct pointing direction in the absence of an optical feedback signal, with an accuracy similar to that of the FOV.

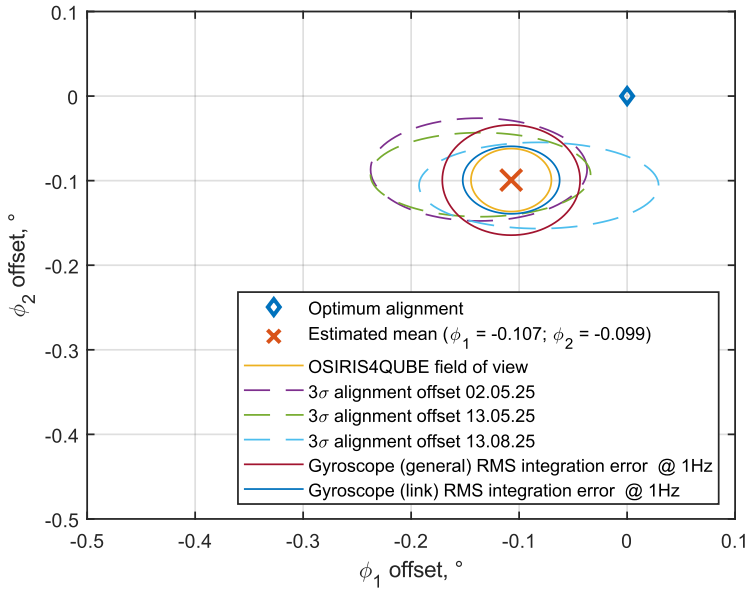

Figure 6. Estimated alignment based on optical tracking and gyroscope measurements.

3.3 Pointing, Acquisition and Tracking Results

To increase the probability of a successful mission, end-to-end tests with the LCT [20] were carried out on the ground in advance. In the next step, the LCT was fully characterised again, integrated in the CubeSat flight model. The influence of micro-vibrations on the optical tracking error was also analysed [21]. Both validation tests served to minimize risk and to rule out performance degradation. Thanks to the precise pointing of the satellite, it was possible to establish a link at the first link attempt,

on the 2nd of May. Figure 7 summarises further link attempts and indicates statistics over several overflights, in order to gain insights into reliability.

Out of a total of 19 attempts in 2025 in total nine were successful, meaning that an optical tracking lock was achieved at 47% of the overpasses. The longest tracking time on the 13th of May was 7 minutes and 25 seconds, which means a 97.5% tracking ratio with a brief interruption, as described later. The mean tracking ratio across all nine links is 71.2%.

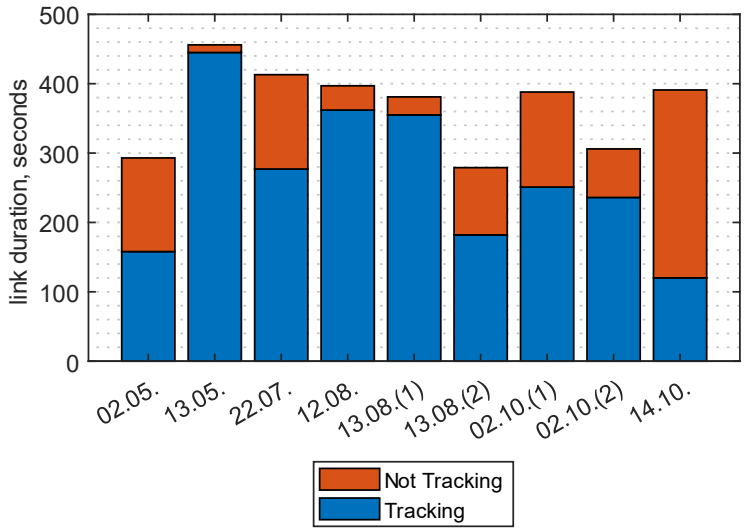

Figure 7. Tracking link statistics over all successful attempts in 2025.

Continuing with a more detailed analysis of successful links, Figure 8 depicts the performance of three links. Figure 8a shows the very first link attempt with successful PAT where the LCT loses the lock shortly after the star tracker readings become invalid (see Figure 2), which is likely due to the high rotation rates needed for 68° of elevation. This happened at about 21:14:00, where all axes show an absolute rotation rate higher than 0.5 °/s.

Figure 8b depicts a link with almost continuous tracking throughout the overpass with an acquisition time of 2 seconds. The interruption is accounted for an overcompensation in the automatic gain control of the optical to electrical signal path, which led to a temporary loss of signal. It is also visible that after an invalid star tracker lock, which occurred around 21:02:15, the rotation rates of all axes indicate a rate higher than 0.3 °/s. The control error of the ADCS (see Figure 3) as well as in the FSM derived boresight error indicate, that the pointing error of the body-pointing increases, while the optical tracking error mean remains at the same magnitude. The tracking lasts 97.5% of the total link time, equivalent to 7 minutes and 25 seconds.

Figure 8c demonstrates a link with 20 degrees maximum elevation angle, where the pointing error of the ADCS was stable, which can be also accounted to an almost constant valid flag of the star tracker (see Figure 4). After 26 seconds needed for acquisition, the link could be established and held until the end of the overflight.

These findings highlight the interplay between elevation angle and tracking performance. While higher elevation angles generally result in larger body-pointing errors, due to increased rotation rates that challenge the employed star tracker, lower elevations yield improved attitude control.

Currently, the optical LCT's tracking error falls behind the anticipated performance. To investigate this behaviour further, the pointing error derived from the FSM is analysed. Closer observation of the signal reveals no strict periodic oscillation. However, error peaks are visible to occur quasi-regularly, at intervals of about 0.5 Hz. Comparing this value with that of the ADCS control loop shows that this update frequency corresponds to the update rate in the target tracking guidance [4].

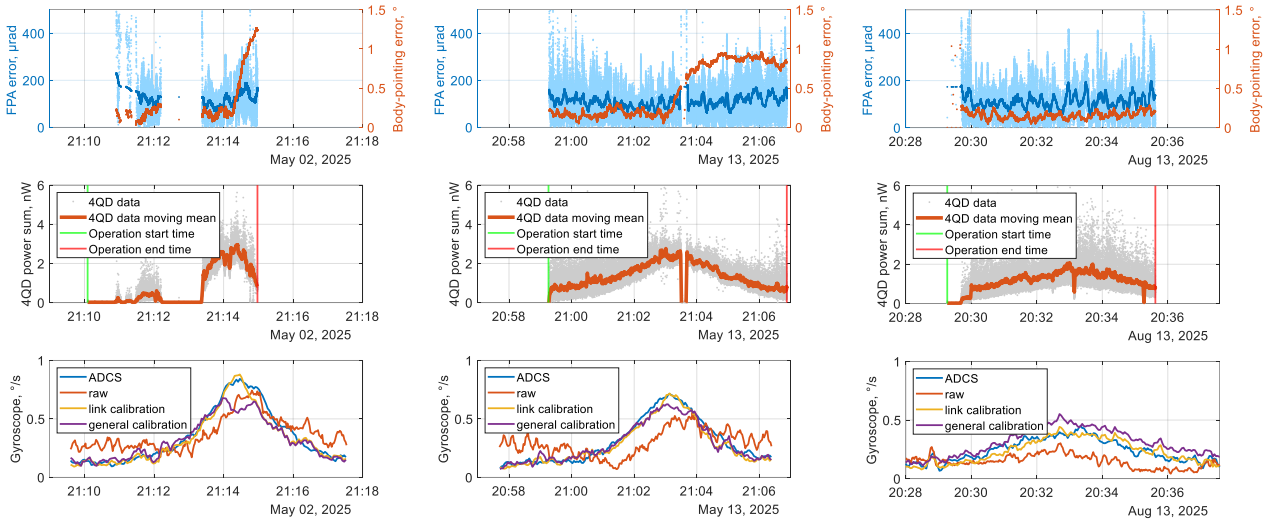

(a) (b) (c)

Figure 8. Tracking at (a) the 2nd of May, (b) the 13th of May and (c) the 13th of August 2025.

To evaluate the control rejection bandwidth required to compensate for the ADCS tracking slew rates relative to the optical axis—known as the pointing instability rate—by the FPA tracking loop, this rate can be derived from the FSM. The PIXL-1 mission encountered pointing instability rates of about 0.05 °/s (3σ) [22]. The LCT itself was designed and tested for up to 0.08 °/s (3σ). Measuring the instability of QUBE, a rate of 0.1047 °/s was calculated.

Therefore, the proposed explanation for the residual LCT pointing error is a combination of the relatively slow target adjustments at 0.5 Hz and the ADCS pointing instability rate being close to the LCT's disturbance rejection bandwidth. The LCT must compensate for errors relating to the optical axes with an additional magnification gain due to the telescope, which can lead to an inherent lag error at the LCT's closed-loop controller at instability rates beyond that specified above. This explanation is further supported by a comparison with an LCT control loop simulation, based on prior system characterisation, depicted in Figure 9.

This simulation shows that reducing the instability rate would improve the performance of the optical link, as it indicates similar mean errors and standard deviations. Measures to reduce optical tracking errors could therefore include making the ADCS controller less aggressive with respect to the optical axes, increasing the target reference update rate to reduce reference error accumulation, increasing the optical FPA tracking bandwidth, or implementing a combination of these measures. These options are being investigated as part of ongoing work.

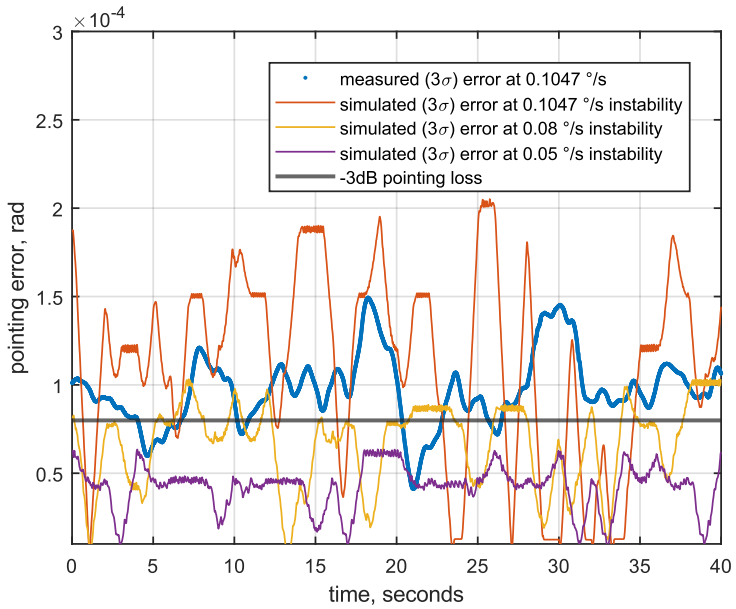

Figure 9. Comparison of actual optical pointing error samples on the QUBE satellite with simulated samples for different body-pointing instability rates.

Nevertheless, the results demonstrate the robustness of the ADCS when it comes to maintaining orientation accuracy across a range of elevation angles. They also highlight the LCT system's capability to sustain effective tracking for almost the entire duration of the link, despite the challenges posed by star tracker-dependent body pointing accuracy. Moreover, the gyroscope's performance paves the way for classical, optical ISLs, such as those in CubeISL. Similarly, the experiments on QUBE are being conducted in preparation of QKD, and thus as a derisking measure for the follow-up project, QUBE-II [23].

4 CONCLUSION

The QUBE mission has shown that the pointing bottleneck of free-space optical communication on small satellites can be mitigated by taking the lessons learned into the design process and using ground tests to validate the performance. Additionally, the OSIRIS4QUBE LCT was used as a precursor, not only for QKD missions, but also to verify a self-contained gyroscope essential to upcoming optical ISL missions. An on-orbit calibration reduced the gyroscope's bias and scale errors to RMS values down to 0.11 °/s. Propagating this calibrated attitude estimate with 1 Hz resets at the LCT's scan rate keeps the pointing knowledge error close to the FOV, but certainly within the FOR of the FPA, effectively bridging the gap between the ADCS's low-frequency attitude estimates and the disturbances that will dominate acquisition during ISLs. Which, in turn, will enable compensation of body-pointing instabilities by feed-forward compensation to the FSM.

In 2025, QUBE successfully established nine optical links out of 19 overpasses thanks to its robust ADCS pointing, which reliably produced pointing residuals below ±0.2°. The mean optical tracking-to-operation time ratio was 71%, with acquisition times as short as two seconds. These results pave the way for autonomous, high-throughput optical links on future CubeSat constellations and QKD missions.

5 ACKNOWLEDGMENTS

The project on which this report is based was funded by the Federal Ministry of Research, Technology and Space under the funding code 16KIS0767. The authors are responsible for the content of this publication.

6 REFERENCES

[1] H. Hemmati, *Near-Earth laser communications,* Second edition, CRC Press, Boca Raton, 2021.
[2] R. Rüddenklau, G. Schitter, *Optimisation of acquisition patterns for establishing inter CubeSat optical communications*, J. Opt. Commun. Netw. (2024).
[3] S.V. Weston, C.D. Burkhard, J.M. Stupl, R.L. Ticknor, B.D. Yost and R.A. Austin et al., *State-of-the-art small spacecraft technology*, 2025.
[4] L. Elsner, T. Petermann, M. von Arnim, K. Schilling, *Pre-flight verification of the CubeSat attitude control system for the QUBE mission*, in: Small Satellites Systems and Services Symposium (4S 2024): 27-31 May 2024, Palma de Mallorca, Spain, Palma de Mallorca, Spain, 2025, p. 155.
[5] S. Li, M. Zhong, *High-Precision Disturbance Compensation for a Three-Axis Gyro-stabilized Camera Mount*, IEEE/ASME Transactions on Mechatronics 20 (2015) 3135–3147.
[6] F. Dell'Olio, T. Natale, Y.-C. Wang, Y.-J. Hung, *Miniaturization of Interferometric Optical Gyroscopes: A Review*, IEEE Sensors J. 23 (2023) 29948–29968.
[7] M. Heimann, M. Liesegang, N. Arndt-Staufenbiel, H. Schröder, K.-D. Lang, *Optical system components for navigation grade fiber optic gyroscopes*, 2013, 88991A.
[8] Z. Shukri, H. Rezaei, M. Fasihanifard, S. Ghofrani, J. Bissonnette, T. Gravey et al., *Photonic integrated circuit microchip-based optical gyroscopes for high-precision inertial measurement units*, in: Integrated Optics: Devices, Materials, and Technologies XXIX, San Francisco, United States, 2025 - 2025, p. 25.
[9] K.M. Riesing, C.M. Schieler, J.S. Chang, N.C. Gilbert, A.J. Horvath, R.S. Reeve et al., *On-orbit results of pointing, acquisition, and tracking for the TBIRD CubeSat mission*, in: Free-Space Laser Communications XXXV: 30 January-1 February 2023, San Francisco, California, United States, San Francisco, United States, 2023, p. 4.
[10] C. Fuchs, F. Moll, D. Giggenbach, C. Schmidt, J. Keim, S. Gaisser, *OSIRISv1 on Flying Laptop: Measurement Results and Outlook*, in: 2019 IEEE International Conference on Space Optical Systems and Applications (ICSOS), Portland, OR, USA, 2019, pp. 1–5.
[11] B. Rödiger, C. Schmidt, *In-orbit demonstration of the world's smallest laser communication terminal: OSIRIS4CubeSat/CubeLCT*, in: Small Satellites Systems and Services Symposium (4S 2024): 27-31 May 2024, Palma de Mallorca, Spain, Palma de Mallorca, Spain, 2025, p. 16.
[12] O. Čierny, K.L. Cahoy, *On-orbit beam pointing calibration for nanosatellite laser communications*, Opt. Eng. 58 (2019) 1.
[13] B. Rödiger, C. Roubal, F. Rein, R. Rüddenklau, A.M. Vishwanath, C. Schmidt, *OSIRIS4CubeSat—The World's Smallest Commercially Available Laser Communication Terminal*, Aerospace 12 (2025) 655.
[14] C. Menninger, F. Moll, B. Rödiger, *Dual wavelength optical system for multiple quantum communication transmitters in Cubesat platform*, in: International Conference on Space Optics - ICSO 2020, Online Only, France, 2021, p. 201.
[15] J.R. Nonay, R. Rüddenklau, A. Sinn, J.P. Jakobs, J. Berlitz, B. Rödiger et al., *Horizontal free-space optical link with CubeISL over 143 km*, J. Opt. Commun. Netw. 16 (2024) 593.
[16] T. Petermann, L. Elsner, B. Schmidt, D. Pearson, T. Datar, I. Mammadov et al., *QUBE-I Mission Update: First Year of Operation of a 3U CubeSat for Quantum-Key-Distribution*

Experiments, in: IAF Space Communications and Navigation Symposium, Sydney, Australia, 2025, pp. 1081–1096.
[17] L. Elsner, J. Dauner, B. Schmidt, T. Petermann, M. Unnikrishnan, R. Rüddenklau et al., *Beacon-Enhanced Attitude Control using Optical Communication Terminals: Design and Validation in the QUBE Mission*, IFAC-PapersOnLine 59 (2025) 115–120.
[18] R. Rüddenklau, S. Barone, E. Garbagnati, S. Spier, G. Schitter, *Feed-forward compensation of body-pointing uncertainties for laser communication terminals*, Journal of Guidance, Control, and Dynamics (2026 [in press]).
[19] S. Poddar, V. Kumar, A. Kumar, *A Comprehensive Overview of Inertial Sensor Calibration Techniques*, Journal of Dynamic Systems, Measurement, and Control 139 (2017).
[20] B. Rödiger, R. Rüddenklau, A. Morab Vishwanath, C. Roubal, F. Moll, C. Fuchs, *Verification of laser communication terminals for CubeSats as preparation for missions PIXL-1 and QUBE under atmospheric conditions*, in: 75th International Astronautical Congress, IAC 2024, 2024.
[21] R. Rüddenklau, B. Rödiger, C. Roubal, C. Schmidt, F. Moll, *Vibration load compliance of a miniaturized CubeSat quantum communication terminal*, Journal of Vibration and Control (2025).
[22] R. Rüddenklau, F. Rein, C. Roubal, B. Rödiger, C. Schmidt, *In-orbit demonstration of acquisition and tracking on OSIRIS4CubeSat*, Optics express 32 (2024) 41188–41200.
[23] C. Roubal, L.R. Rodeck, P. Gagern, J.P. Jakobs, *Optical design of the CubeSat-based QKD terminal QUBE-II*, in: Free-Space Laser Communications XXXVIII, San Francisco, United States, 2026 - 2026, p. 63.